Inorganic Chemistry

Article

pubs.acs.org/IC

Mercury-Modulated Supramolecular Assembly of a Hexaphenylbenzene Derivative for Selective Detection of Picric Acid

Vandana Bhalla,* Sharanjeet Kaur, Varun Vij, and Manoj Kumar*

Department of Chemistry, UGC Sponsored-Centre for Advanced Studies I, Guru Nanak Dev University, Amritsar 143005, Punjab, India

Supporting Information

ABSTRACT: Spherical aggregates of hexaphenylbenzene derivative **5** undergo metal-induced modulation to form nanorods in the presence of Hg^{2+} ions, which exhibit selective and sensitive response toward picric acid (PA) with a detection limit of 6.87 ppb.

INTRODUCTION

Recently, the development of cost-efficient, selective, portable, fast, and sensitive methods for the detection of nitro derivatives has attracted great research interest.[1] Trace detection of explosives is very important in combating terrorism,[2,3] for maintaining national security, and for providing environmental safety.[4] Fluorescence signaling is one of the first choices among various methods used for the detection of nitro derivatives because of its high sensitivity and selectivity.[5] To date, various fluorescent chemosensors, fluorescent polymers, and nanoparticles have been developed for the detection of nitro derivatives.[6] Most of these fluorogenic chemosensors for various nitro derivatives are either less selective or exhibit low-to-moderate Stern−Volmer constants. In the present scenario, the use of metal centers for the coordination of analytes has offered an alternative strategy for the design of chemosensors because the stereochemical preferences of transition-metal ions can impart selective binding tendencies toward analytes.[7] Among various nitro derivatives, the detection of picric acid (PA) is important because of its wide usage in the manufacture of rocket fuels, fireworks, deadly explosives, and sensitizers in photographic emulsions and as a component in matches, etc.[8] PA was used in medicinal formulations in the treatment of malaria, trichinosis, herpes, smallpox, and antiseptics.[9] In metallography laboratories, PA is widely used for the common steel etchant known as picral. PA is reportedly more dangerous in the dehydrated state, which can undergo spontaneous detonation to cause explosion. Further, PA has also been recognized as an environmental contaminant and is harmful to wildlife and humans.[10] In spite of the awareness about the adverse effects of PA, the compound has probably been released to the environment during the manufacture of explosives and in loading, assembly, and packing activities at military installations. Although the explosive power of PA is superior to that of 2,4,6-trinitrotoluene (TNT), less attention has been paid to the development of methods for the selective detection of PA. In the past few years, many molecular and modulated chemosensors specifically for PA have been reported. Patil and co-workers[6c] have reported a fluoranthene-based fluorescent chemosensor, which detects PA by intercalative $\pi-\pi$ interaction and exhibits good quenching efficiency. In another work, Mukherjee and co-workers[6d] have used small discrete and easily synthesizable molecules for PA detection. They have also used metal-induced self-assembled three-dimensional trigonal prisms[11] and cages[12] for fluorogenic detection of PA. In addition to these, Tang[13] and Fang[14] and co-workers have explored fluorescent molecules in their aggregated and self-assembled states, respectively, for the detection of PA among other analogues. Recently, we reported an (*N*,*N*-dimethylamino)cinnamaldehyde-based Hg^{2+} ensemble that behaves as a chemosensor for PA mainly in organic media with a poor detection limit and a moderate quenching constant.[15] Although there are many reports on the molecular recognition of PA, the combination of high selectivity, very low detection limit, and high quenching constant is still the major requirement for materialization of PA sensors. Thus, to overcome such problems, we have now designed and synthesized hexaphenylbenzene derivative **5** having imine linkages, which exhibits aggregation-induced emission enhancement (AIEE) in a mixed aqueous medium because of the presence of free rotors[16] to give fluorogenic aggregates. Interestingly, these aggregates of derivative **5** have a strong affinity for Hg^{2+} ions and undergo metal-induced modulation in

Received: November 2, 2012
Published: April 24, 2013

   dx.doi.org/10.1021/ic3023997 | *Inorg. Chem.* 2013, 52, 4860−4865

Scheme 1. Synthesis of Compound 5[a]

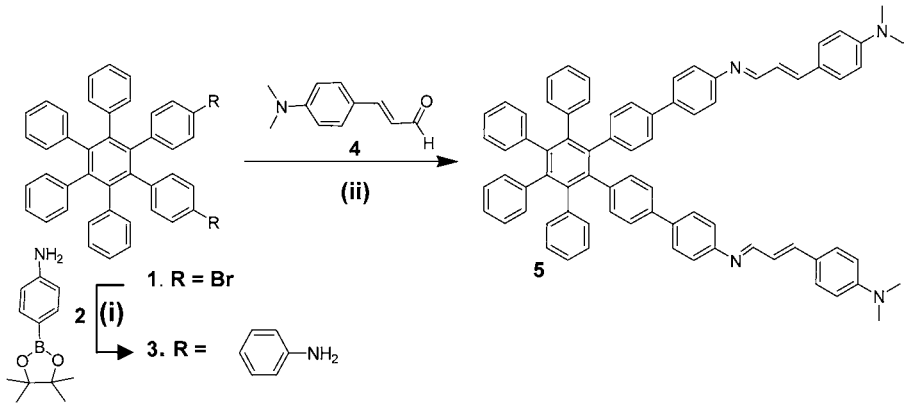

[a](i) THF, K_2CO_3(aq), $PdCl_2(PPh_3)_2$; (ii) THF/EtOH (3:1).

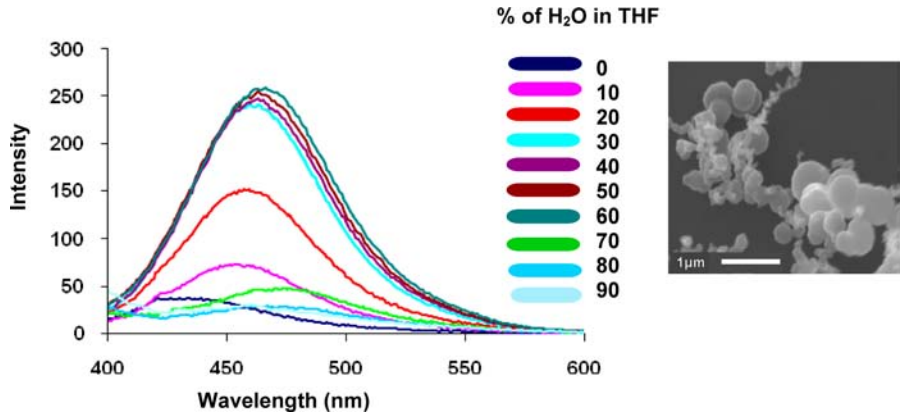

Figure 1. Fluorescence emission spectra of **5** (5 μM) in different ratios of H_2O/THF at λ_{ex} = 380 nm. Inset: SEM images of aggregates of compound **5** in H_2O/THF (4:6).

the presence of Hg^{2+} ions. In addition, supramolecular assemblies of the **5**-Hg^{2+} ensemble behave as highly selective chemosensors for PA with very low detection limits and very high quenching constants. Besides, we have used these metal-induced aggregates for the fabrication of fluorescent paper strips, which can be helpful for the practical detection of traces of PA. To the best of our knowledge, this is the first report where supramolecular assemblies of mercury ensembles of AIEE active hexaphenylbenzene derivatives have been utilized for the sensitive and selective detection of PA among various analogues.

RESULTS AND DISCUSSION

The Suzuki–Miyaura cross-coupling of compound **1**[17] with boronic ester **2**[18] furnished compound **3** in 53% yield, which upon condensation with (*N*,*N*-dimethylamino)cinnamaldehyde (**4**) in tetrahydrofuran (THF)/ethanol (EtOH) (3:1) furnished compound **5** in 63% yield (Scheme 1). The structures of compounds **3** and **5** were confirmed from their spectroscopic and analytical data (Supporting Information, Figures S1–S6). The ^{1}H NMR spectrum of compound **5** showed one singlet at 2.96 ppm corresponding to $N(CH_3)_2$ protons, two doublets at 6.68 and 8.21 ppm corresponding to aromatic protons and N=CH protons, respectively, two multiplets at 6.85–7.01 and 7.05–7.09 ppm both corresponding to CH and aromatic protons, and two multiplets at 7.13–7.15 and 7.24–7.45 ppm corresponding to aromatic protons. A parent ion peak for M + H^+ was observed at *m*/*z* 1031.5050 in the electrospray ionization mass spectrometry (ESI-MS) spectrum. These spectroscopic data corroborate the structure of **5**.

The UV–vis absorption spectrum of compound **5** in THF exhibits absorption bands at 290 and 380 nm. However, in the presence of 40% H_2O in THF, both of the absorption bands are slightly red-shifted along with the appearance of a leveling-off tail in the visible spectral region, which may be attributed to the formation of nanoaggregates[19] (Supporting Information, Figure S7). The formation of aggregates of derivative **5** was supported by a scanning electron microscopy (SEM) image of compound **5** in H_2O/THF (4:6), which shows the presence of spherical nanoaggregates (Figure 1, inset).

In the fluorescence spectrum, compound **5** exhibits a weak fluorescence emission at 460 nm (ϕ_0 = 0.03)[20] when excited at λ_{ex} = 380 nm. However, a subsequent increase of the volume fraction of water up to 60% leads to enhancement of the emission intensity (ϕ = 0.48; Figure 1). However, the addition of a water fraction higher than 60% leads to a decrease in the emission intensity. We believe that in aqueous media intramolecular rotations are restricted because of the formation of aggregates, which block the nonradiative channels and populate the radiative excitons, thereby making the molecule emissive in their aggregated state. A decrease in the emission intensity upon the addition of more than a 60% water fraction may be attributed to the low solubility of derivative **5** in the solvent mixture, thus leading to a decrease in the number of

dx.doi.org/10.1021/ic3023997 | Inorg. Chem. 2013, 52, 4860–4865

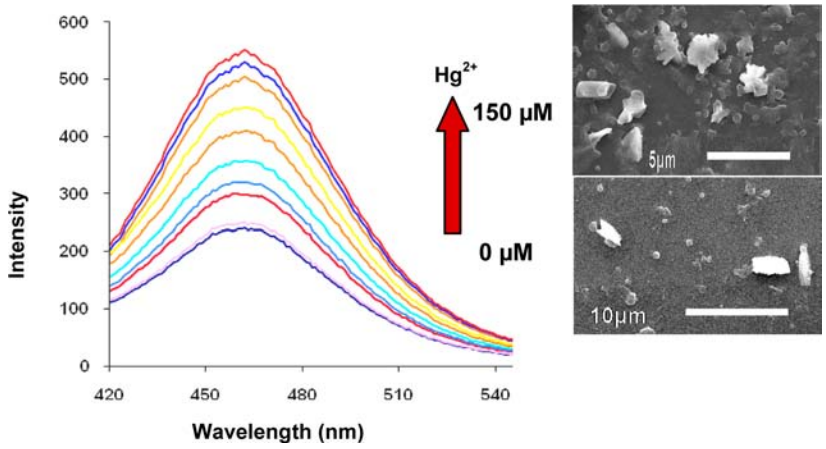

Figure 2. Fluorescence spectra of **5** (5 μM) in the presence of Hg^{2+} ions (0−150 μM) in H_2O/THF (4:6) at λ_{ex} = 380 nm and SEM images of a **5**-Hg^{2+} ensemble in H_2O/THF (4:6).

emissive molecules per unit volume. Because the decreasing trend in the intensity caused by the smaller number of emitting molecules governs over the fluorescence enhancement due to the restriction-in-rotation process, the net fluorescence intensity is decreased.[21]

To verify the mechanism of restriction in rotation, we recorded the fluorescence spectra of compound **5** in highly viscous glycerol. As expected, the solution of compound **5** becomes more emissive because of increased viscosity, which hampers the intramolecular rotations[22] (Supporting Information, Figure S8). Further, the concentration-dependent emission study of compound **5** in THF exhibits a nonlinear increase in the emission intensity with an increase in the concentration (Supporting Information, Figure S9, inset), which supports the theory that emission enhancement is due to the aggregation mechanism instead of normal concentration-dependent emission (Supporting Information, Figure S9) and thus proves the mechanism.

The presence of imine linkages in derivative **5** prompted us to evaluate its binding behavior toward different metal ions using UV−vis and fluorescence spectroscopy. The titration experiments were carried out in H_2O/THF (4:6) by adding aliquots of different metal ions (Cu^{2+}, Fe^{2+}, Fe^{3+}, Hg^{2+}, Co^{2+}, Pb^{2+}, Zn^{2+}, Ni^{2+}, Cd^{2+}, Ag^{+}, Ba^{2+}, Mg^{2+}, K^{+}, Na^{+}, and Li^{+}) as their perchlorate salts. Upon the addition of Hg^{2+} ions (0−250 μM) to the solution of aggregates of compound **5**, the absorption spectrum exhibits an increase in the absorption intensity of a leveling-off tail in the visible spectral region (Supporting Information, Figure S10),[23] thus indicating interaction between aggregates of derivative **5** and Hg^{2+} ions to generate metal-modulated aggregates. The solution containing aggregates was visibly transparent and stable at room temperature for several weeks. Upon the addition of Hg^{2+} ions (0−150 μM) to the solution of aggregates of derivative **5**, a significant emission enhancement (7.14-fold) in the fluorescence spectrum is observed (ϕ = 0.72; Figure 2).

We believe that the presence of Hg^{2+} ions further rigidifies the molecule and restricts the rotational relaxation of the excited state via nonradiative modes, thus resulting in emission enhancement. This metal-induced modulation was also supported by SEM images of a compound **5**-Hg^{2+} ensemble in H_2O/THF (4:6), which show the presence of rodlike morphology (Figure 2, inset). This observation clearly suggests interaction between aggregates and Hg^{2+} ions, thus leading to modulation of the self-assembled structure of derivative **5** in aqueous media. These results are also in agreement with the emission enhancement observed in fluorescence studies. The detection limit of aggregates of **5** as a fluorescent chemosensor for the analysis of Hg^{2+} ions was found to be 35.9 ppb (Supporting Information, Figure S11). Further, to test the reversibility of the proposed complexation, we carried out a reversibility experiment. The addition of tetrabutylammonium acetate (TBAOAc) to the solution of **5**-Hg^{2+} (5 μM) in H_2O/THF (4:6) restores the fluorescence of aggregates of derivative **5**. This decrease in the fluorescence intensity is due to the strong affinity of acetate ions for Hg^{2+} ions, which is responsible for decomplexation of the **5**-Hg^{2+} complex; hence, Hg^{2+} ions are not available for binding with a receptor. The further addition of Hg^{2+} ions revives the respective fluorescence emission, thus indicating the reversible behavior of derivative **5** for Hg^{2+} ions (Supporting Information, Figure S12). However, no significant change in the fluorescence spectrum was observed in the presence of other metal ions such as Co^{2+}, Pb^{2+}, Zn^{2+}, Ni^{2+}, Cd^{2+}, Ag^{+}, Ba^{2+}, Mg^{2+}, K^{+}, Na^{+}, and Li^{+} [Supporting Information, Figure S13 (series 1)]. To test the practical applicability of compound **5** as a Hg^{2+} selective sensor, competitive experiments were carried out in the presence of Hg^{2+} ions at 150 μM mixed with the other metal ions at 500 μM [Supporting Information, Figure S13 (series 2)]. No significant variation in the fluorescence intensity was found by comparisons with and without other metal ions. Fitting the changes in the fluorescence spectra of compound **5** with Hg^{2+} ions using the nonlinear regression analysis program *SPECFIT*[24] gave a good fit and demonstrated that 1:1 stoichiometry (host/guest) was the most stable species in the solution with the binding constant (log β) = 9.83 with 73% complexation. The binding of Hg^{2+} ions with receptor **5** is also proven by mass spectrometry (Supporting Information, Figure S14), which shows the parent peak at m/z 1453.8758 corresponding to the **5**+Hg^{2+}+2ClO_4^-+Na^+ complex. This not only confirms the binding of Hg^{2+} ions with receptor **5** but also proves the 1:1 stoichiometry of host and guest species. Further, the 1:1 metal/receptor stoichiometry was also confirmed by Job's plot (Supporting Information, Figure S15). To elucidate the binding mode of **5** with Hg^{2+} ions, the ^{1}H NMR spectrum of its complex with Hg^{2+} ions was also recorded. Upon the addition of Hg^{2+} ions (150 μM) to the solution of **5**, the downfield shift of 0.4 ppm in the imino

dx.doi.org/10.1021/ic3023997 | *Inorg. Chem.* 2013, 52, 4860−4865

protons was observed, which indicates interaction between derivative **5** and Hg^{2+} ions (Supporting Information, Figure S16).

The strong emission of nanoaggregates of the **5**-Hg^{2+} ensemble prompted us to explore their potential application as a "chemosensing ensemble" for the detection of various nitro derivatives. To investigate the properties of the compound **5**-Hg^{2+} ensemble for recognition of nitro derivatives, we carried out fluorescence titrations of the **5**-Hg^{2+} ensemble (5 μM) in a H_2O/THF (4:6) mixture with various nitro derivatives such as PA, TNT, 2,4-dinitrotoluene (DNT), 1,4-dinitrobenzene (DNB), 1,4-dinitrobenzoic acid, nitromethane, 2,3-dimethyl-2,3-dinitrobutane, 1,4-benzoquinone, and benzoic acid. The UV–vis absorption studies of aggregates of the **5**-Hg^{2+} ensemble in the presence of increasing amounts of PA (15 equiv) in H_2O/THF (4:6) show a diminishing in the leveling-off tail in the visible region with the appearance of an isosbestic point at 460 nm (Supporting Information, Figure S17). In the fluorescence studies, quenching of the fluorescence emission is observed upon the addition of 75 μM PA (Figure 3). The

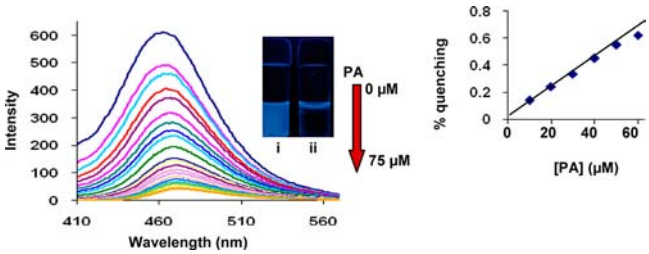

Figure 3. Change in the fluorescence of **5**-Hg^{2+} (5 μM) upon the addition of PA (75 μM) in H_2O/THF, (4:6); λ_{ex} = 380 nm. Inset: difference in the fluorescence of **5** (i) before and (ii) after the addition of PA to the **5**-Hg^{2+} ensemble; Stern–Volmer plot of the percent quenching of the **5**-Hg^{2+} complex versus the concentration of PA (μM).

Stern–Volmer plot of the change in the intensity of aggregates of **5**-Hg^{2+} with respect to the PA concentration is linear (Figure 3, inset) and gives a quenching constant (K_{SV})[25] of 1.92×10^5 M^{-1}. Thus, the quenching of the fluorescence of aggregates of the **5**-Hg^{2+} ensemble upon the addition of PA is ascribed to the static quenching (Figure 3). The detection limit was found to be 6.87 ppb. The quenching constant and detection limit of the **5**-Hg^{2+} ensemble toward PA are noticeably higher than those reported in previous reports.[26]

Interestingly, the **5**-Hg^{2+} ensemble exhibits remarkable selectivity toward PA among other nitro derivatives, whereas under similar conditions, aggregates of derivative **5** in the absence of Hg^{2+} ions do not exhibit a selective response toward PA (Supporting Information, Figure S18). This indicates the importance of the Hg^{2+} ensemble of derivative **5** for discrimination of PA from other analogous nitro derivatives. The PA, being a strong acid, has a great tendency to transfer protons of hydroxyl groups to the basic *N*,*N*-dimethylamino group to make an electrostatic complex between host and guest (Scheme 2). This strong complexation between the **5**-Hg^{2+} ensemble and PA facilitates electron transfer from the excited hexaphenylbenzene to the lowest unoccupied molecular orbital (LUMO) of PA so as to shift the electron to a nonradiating decay path and quench fluorescence emission.

To verify the mechanism of quenching, we analyzed the effect of the pH on the quenching efficiency using a *N*-(2-

Scheme 2. Quenching Mechanism of Emission of 5-Hg^{2+} with PA

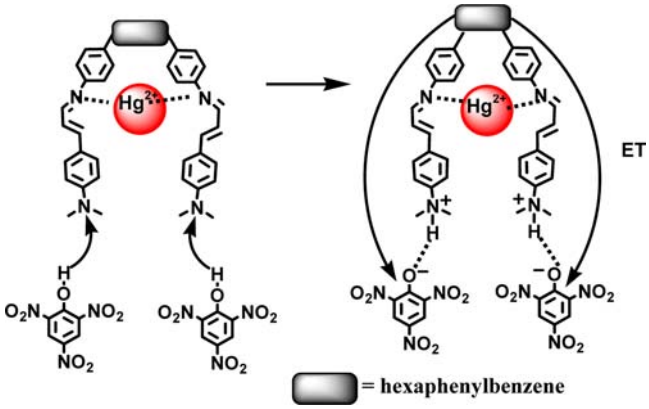

hydroxyethyl)piperazine-*N*′-2-ethanesulfonic acid buffer. At acidic pH 6, the quenching in emission of the **5**-Hg^{2+} ensemble is only 80%, which is considerably less than the percent quenching (95%) at neutral pH. At low pH, the electrostatic interactions between the complex and PA are weakened because of already protonated *N*,*N*-dimethylamino groups. As a result, the electrostatic interactions between the **5**-Hg^{2+} ensemble and PA are inhibited and electron transfer from hexaphenylbenzene to PA is constrained. However, no substantial effect on the quenching efficiency was observed at higher pH (Supporting Information, Figure S19). To confirm the quenching mechanism, we carried out ^1H NMR spectrometry of the **5**-Hg^{2+} ensemble in the presence of PA, which shows a downfield shift of 0.12 ppm in the signal of methyl protons (from 3.00 to 3.12 ppm) of the *N*,*N*-dimethylamino group (Supporting Information, Figures S20 and S21). This shift is due to protonation of the nitrogen atom of the *N*,*N*-dimethylamino groups by PA, thus leading to deshielding of the methyl protons. To verify the protonating sites in the free ligand, we also carried out the ^1H NMR spectrometry of compound **5** in the presence of trifluoroacetic acid, which shows a downfield shift of 0.2 ppm in the signals of methyl protons of the *N*,*N*-dimethylamino groups, whereas no shift in the signal of imino protons was observed (Supporting Information, Figure S22). This confirms that the nitrogen atom of the *N*,*N*-dimethylamino group is the only plausible site available for protonation, thus confirming the proposed quenching mechanism (Scheme 2).

Because the presumed quenching mechanism is electrostatic in the case of PA, we examined the interference of various anions (F^-, Cl^-, Br^-, I^-, AcO^-, NO_3^-, CN^-, $H_2PO_4^-$, and ClO_4^-) toward the interaction of PA with the **5**-Hg^{2+} ensemble by adding PA to the solution of the **5**-Hg^{2+} ensemble (H_2O/THF, 4:6) followed by the addition of various anions. However, no substantial effect on the emission intensity was observed, which shows the negligible interference by anions in the quenching mechanism of PA (Supporting Information, Figure S23).

Further, the greater selectivity of the Hg^{2+} ensemble of derivative **5** toward PA may also be attributed to easier electron transfer from a photoexcited **5**-Hg^{2+} complex to the LUMO of PA (−3.8 eV)[27] than from photoexcited **5** to the LUMO of PA because of the lower energy of the LUMO of the **5**-Hg^{2+} complex (−3.21 eV) compared to the energy of the LUMO of derivative **5** (−3.03 eV; Supporting Information, Figure S24).

dx.doi.org/10.1021/ic3023997 | *Inorg. Chem.* 2013, 52, 4860–4865

However, the net energy band gaps for compound **5** and ensemble **5**-Hg^{2+} are calculated from their respective UV−vis absorption spectra, which turned out to be 2.61 and 2.58 eV, respectively, which show that there is a negligible change (0.03 eV) in the energy band gaps of **5** and **5**-Hg^{2+} (Supporting Information, Figure S25).[28] Thus, no considerable shift in the emission wavelength of compound **5** was observed upon the addition of Hg^{2+} ions in Figure 2.

We also studied the quenching mechanism of the emission of aggregates of the **5**-Hg^{2+} ensemble with other nitro derivatives (TNT, DNT, DNB, etc.). These nitro derivatives also exhibit linear Stern−Volmer plots (Supporting Informarion, Figure S26), which favor static quenching due to charge transfer between photoexcited hexaphenylbenzene and electron-withdrawing nitro derivatives. To confirm this mechanism, we compared the energy of the LUMO of the **5**-Hg^{2+} ensemble with LUMOs of these nitro derivatives and found that the LUMO of the former is relatively higher in energy than those of the latter[27,29] (TNT = −3.7 eV, DNT = −3.5 eV, and DNB = −3.35 eV), which facilitates charge transfer between the donor and acceptor groups. However, because of the lack of tendency to protonate the *N*,*N*-dimethylamino group, other nitro derivatives do not follow the ionic mechanism, which reduces their quenching efficiency in comparison to PA. In addition, because no spectral overlap was observed between the emission spectrum of **5**-Hg^{2+} and absorption spectra of these nitro derivatives, the possibility of an energy-transfer mechanism was diminished (Supporting Information, Figure S27).

During the preparation and packaging of explosive devices, nitro derivatives can contaminate the human body, clothing, and other materials in the surroundings.[30] In this context, we prepared test strips by dip-coating solutions of aggregates of the **5**-Hg^{2+} ensemble in H_2O/THF (4:6) on Whatman filter paper followed by drying the strips under vacuum to test the residual contamination in contact mode.

We performed the paper strip test on the **5**-Hg^{2+} ensemble in contact mode, and fluorescence quenching was observed upon dipping of the test strips into a solution of PA (229 ppm; Figure 4A). We also checked the effect of various concentrations of a PA solution on the fluorescent paper strip by applying small spots of different concentrations of PA to the test strips. The formation of dark spots of different strengths shows that regulation of the quenching behavior of PA is practically applicable by varying the concentration of PA even up to 0.229 ppb (Figure 4B). These results show the practical applicability of a mercury ensemble for the instant visualization of traces of PA.

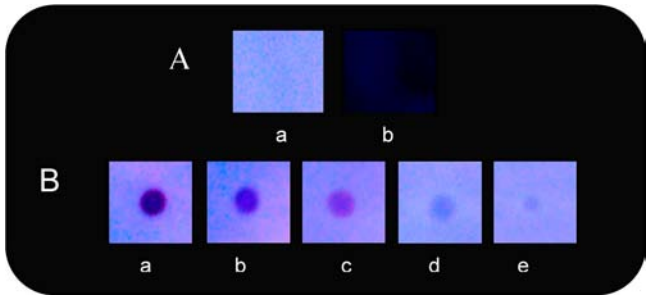

Figure 4. Paper strip test. (A) (a) Before and (b) after dipping of the test strips of the **5**-Hg^{2+} ensemble into a PA solution (10^{-3} M in THF). (B) Application of small spots of different concentrations of PA [(a) 229 × 10^3 ppm, (b) 229 ppm, (c) 2.29 ppm, (d) 22.9 ppb, and (e) 0.22 ppb] on the test strips of the **5**-Hg^{2+} ensemble. All images were taken under 365 nm UV illumination.

CONCLUSION

We designed and synthesized hexaphenylbenzene-based derivative **5** having AIEE characteristics. The aggregates of derivative **5** undergo modulation in the presence of Hg^{2+} ions to form nanorods. Interestingly, supramolecular assemblies of the **5**-Hg^{2+} ensemble work as an efficient and sensitive fluorescent chemosensor for PA at the ppb level. In addition, the present study demonstrates the utility of solution-coated dip strips of the **5**-Hg^{2+} ensemble for the trace detection of PA.

EXPERIMENTAL SECTION

General Experimental Methods. All metal perchlorates were purchased from Aldrich and were used without further purification. Potassium carbonate, ethanol, and tetrabutylammonium salts of anions were purchased from Sigma Aldrich. THF was dried over sodium metal and benzophenone before it was used for analytical studies. All of the fluorescence spectra were recorded on a Shimadzu 5301 PC spectrofluorimeter. UV−vis absorption spectra were recorded on a Shimadzu UV-2450PC spectrophotometer with a quartz cuvette (path length: 1 cm). The cell holder was thermostatted at 25 °C. Elemental analysis was done using a Flash EA 1112 CHNS/O analyzer of Thermo Electron Corp. ^{1}H and ^{13}C NMR spectra were recorded on JEOL-FT NMR-AL 300 MHz and Bruker (Avance II) FT-NMR 400 MHz spectrophotometers using $CDCl_3$ and dimethyl-d_6 sulfoxide as solvents and tetramethylsilane [$Si(CH_3)_4$] as an internal standard. Data are reported as follows: chemical shifts in parts per million (δ), multiplicity (s = singlet, br = broad signal, d = doublet, and m = multiplet), coupling constants (Hz), integration, and interpretation. All spectrophotometric titration curves were fitted with *SPECFIT 32* software.

Experimental Details of Finding the Detection Limit. To determine the detection limit, fluorescence titration of compound **5** with Hg^{2+} ions was carried out by adding aliquots of a mercury solution of micromolar concentration and plotting the fluorescence intensity as a function of Hg^{2+} ions. From this graph, the concentration at which there was a sharp change in the fluorescence intensity multiplied with the concentration of receptor **5** gave the detection limit.

Syntheses. Compounds **1**[17] and **2**[18] were synthesized according to literature procedures.

*Synthesis of 1,2-Bis[4-amino-(1,1′-biphenyl)-4′-yl]-3,4,5,6-tetraphenylbenzene (**3**).* To a solution of **1** (0.3 g, 0.43 mmol) and **2** (0.23 g, 1.08 mmol) in THF were added K_2CO_3 (0.48 mg, 3.5 mmol), distilled H_2O (3 mL), and [$Pd(Cl)_2(PPh_3)_2$] (0.12 g, 0.17 mmol) under argon, and the reaction mixture was refluxed overnight. THF was then removed under vacuum, and the residue so obtained was treated with water, extracted with dichloromethane, and dried over anhydrous Na_2SO_4. The organic layer was evaporated, and the compound was purified by column chromatography using ethyl acetate as an eluent to give compound **3**, which was further recrystallized from methanol to provide 0.58 g of a white solid (yield 53%). Mp: 220 °C. ^{1}H NMR (300 MHz, $CDCl_3$): δ 3.61 (br, 4H, NH_2), 6.64 (d, 4H, J = 9 Hz, ArH), 6.81−6.85 (m, 24H, ArH), 7.05 (d, 4H, J = 9 Hz, ArH), 7.24 (d, 4H, J = 9 Hz, ArH). ^{13}C NMR (75 MHz, $CDCl_3$): δ 80.51, 118.52, 124.77, 125.14, 125.20, 126.54, 126.64, 127.15, 127.20, 131.42, 131.84, 135.47, 136.87, 137.25, 139.35, 139.58, 140.42, 140.57, 140.62, 152.61. ESI-MS: m/z 717 [$(M + 1)^+$]. Anal. Calcd for $C_{54}H_{40}N_2$: C, 90.47; H, 5.62; N, 3.91. Found: C, 90.42; H, 5.66; N, 3.87.

*Synthesis of 1,2-Bis[4-(3-iminoprop-1-en-1-yl)-N,N-dimethylaniline-(1,1′-biphenyl)-4′-yl]-3,4,5,6-tetraphenylbenzene (**5**).* A clear solution of compounds **3** (0.06 g, 0.083 mmol) and **4** (0.03 g, 0.16 mmol) in 5 mL of dry THF/C_2H_5OH (3:1) was stirred at 60 °C. After the reaction mixture was stirred for 36 h, the solvent was evaporated under reduced pressure and dry methanol was poured into it. The solid was filtered and washed with methanol to afford compound **5**

dx.doi.org/10.1021/ic3023997 | *Inorg. Chem.* 2013, 52, 4860−4865

(0.0368 g, 63%). The compound was recrystallized in $CHCl_3$/MeOH. ^1H NMR (400 MHz, $CDCl_3$): δ 2.96 (s, 12H, $N(CH_3)_2$), 6.68 (d, 4H, J = 8 Hz, ArH), 6.85−7.01 (m, 2H, CH and 18H, ArH), 7.05−7.09 (m, 2H, CH and 4H, ArH), 7.13−7.15 (m, 8H, ArH), 7.24−7.45 (m, 10H, ArH), 8.21 (d, J = 8 Hz, 2H, N=CH). ^{13}C NMR (100 MHz, $CDCl_3$): δ 40.22, 111.76, 112.01, 118.24, 121.20, 123.24, 123.82, 124.38, 124.86, 125.21, 126.6, 126.71, 127.30, 127.86, 128.17, 130.84, 131.46, 131.70, 131.82, 138.06, 138.63, 140.00, 140.47, 140.68, 151.38, 161.91. ESI-MS: m/z 1030.50 ($M + H^+$). Elem anal. Calcd for $C_{76}H_{62}N_4$: C, 88.51; H, 6.06; N, 5.43. Found: C, 88.54; H, 6.01; N, 5.42.

■ ASSOCIATED CONTENT

Supporting Information

Fluorescence and UV−vis absorption studies, selectivity and competitive graphs, Job's plot, a detection limit plot, a Stern−Volmer plot, cyclic voltammograms, NMR and mass spectral studies of compounds **3** and **5**, and table of a comparison of the present manuscript with previous reports. This material is available free of charge via the Internet at http://pubs.acs.org.

■ AUTHOR INFORMATION

Corresponding Author

*E-mail: vanmanan@yahoo.co.in (V.B.), mksharmaa@yahoo.co.in (M.K.).

Notes

The authors declare no competing financial interest.

■ ACKNOWLEDGMENTS

We are grateful to the DST for financial support (Grants SR/S1/OC-69/2012 and SR/S1/OC-63/2010).

■ REFERENCES

(1) (a) Yinon, J. *Anal. Chem.* **2003**, *75*, 99. (b) Rouhi, A. M. *Chem. Eng. News* **1997**, *75*, 14. (c) Steinfeld, J. I.; Wormhoudt, J. *Annu. Rev. Phys. Chem.* **1998**, *49*, 203.

(2) Potyrailo, R. A.; Mirsky, V. M. *Chem. Rev.* **2008**, *108*, 770.

(3) Achyuthan, K. E.; Bergstedt, T. S.; Chen, L.; Jones, R. M.; Kumaraswamy, S.; Kushon, S. A.; Ley, K. D.; Lu, L.; McBranch, D.; Mukundan, H.; Rininsland, F.; Shi, X.; Xia, W.; Whitten, D. J. *J. Mater. Chem.* **2005**, *15*, 2648.

(4) (a) McQuade, D. T.; Pullen, A. E.; Swager, T. M. *Chem. Rev.* **2000**, *100*, 2537. (b) Toal, S. J.; Trogler, W. J. *J. Mater. Chem.* **2006**, *16*, 2871. (c) Germain, M. E.; Knapp, M. J. *Chem. Soc. Rev.* **2009**, *38*, 2543.

(5) (a) Jian, C.; Seit, W. J. *Anal. Chim. Acta* **1990**, *237*, 265. (b) Yang, X.; Niu, C. J.; Shen, G. L.; Yu, R. Q. *Analyst* **2001**, *126*, 349.

(6) (a) Kartha, K. K.; Babu, S. S.; Srinivasan, S.; Ajayaghosh, A. *J. Am. Chem. Soc.* **2012**, *134*, 4834. (b) Liu, X.; Xu, Y.; Jiang, D. *J. Am. Chem. Soc.* **2012**, *134*, 8738. (c) Venkatramaiah, N.; Kumar, S.; Patil, S. *Chem. Commun.* **2012**, *48*, 5007. (d) Shanmugaraju, S.; Joshi, S. A.; Mukherjee, P. S. *J. Mater. Chem.* **2011**, *21*, 9130. (e) Gole, B.; Shanmugaraju, S.; Bar, A. K.; Mukherjee, P. S. *Chem. Commun.* **2011**, *47*, 10046.

(7) (a) Germain, M. E.; Knapp, M. J. *Inorg. Chem.* **2008**, *47*, 9748. (b) Germain, M. E.; Knapp, M. J. *J. Am. Chem. Soc.* **2008**, *130*, 5422. (c) Chow, C. F.; Lam, M. H. W.; Sui, H.; Wong, W.-Y. *Dalton Trans.* **2005**, 475.

(8) (a) Safety Data Sheet for Picric Acid, Resource of National Institutes of Health. (b) Pimienta, V.; Etchenique, R.; Buhse, T. *J. Phys. Chem. A* **2001**, *105*, 10037. (c) Beyer, C.; Bohme, U.; Pietzsch, C.; Roewer, G. *J. Organomet. Chem.* **2002**, *654*, 187.

(9) *Patty's Toxicology*; John Wiley & Sons: New York, 2000; Vol. *IIB*, p 980.

(10) Wyman, J. F.; Serve, M. P.; Hobson, D. W.; Lee, L. H.; Uddin, D. E. *J. Toxicol. Environ. Health* **1992**, *37*, 313.

(11) Shanmugaraju, S.; Jadhav, H.; Patil, Y. P.; Mukherjee, P. S. *Inorg. Chem.* **2012**, *51*, 13072.

(12) Wang, M.; Vajpayee, V.; Shanmugaraju, S.; Zheng, Y. R.; Zhao, Z.; Kim, H.; Mukherjee, P. S.; Chi, K. W.; Stang, P. J. *Inorg. Chem.* **2011**, *50*, 1506.

(13) Lu, P.; Lam, J. W. Y.; Liu, J.; Jim, C. K. W.; Yuan, W.; Xie, N.; Zhong, Y.; Hu, Q.; Wong, K. S.; Cheuk, K. K. L.; Tang, B. Z. *Macromol. Rapid Commun.* **2010**, *31*, 834.

(14) Ding, L.; Liu, Y.; Cao, Y.; Wang, L.; Xin, Y.; Fang, Y. *J. Mater. Chem.* **2012**, *22*, 11574.

(15) Kumar, M.; Reja, S. I.; Bhalla, V. *Org. Lett.* **2012**, *14*, 6084.

(16) Wang, J.; Mei, J.; Yuan, W.; Lu, P.; Qin, A.; Sun, J.; Ma, Y.; Tang, B. Z. *J. Mater. Chem.* **2011**, *21*, 4056.

(17) Terazono, Y.; Liddell, P. A.; Garg, V.; Kodis, G.; Brune, A.; Hambourger, M.; Moore, A. L.; Moore, T. A.; Gust, D. *J. Porphyrins Phthalocyanines* **2005**, *9*, 706.

(18) Bhalla, V.; Tejpal, R.; Kumar, M.; Puri, R. K.; Mahajan, R. K. *Tetrahedron Lett.* **2009**, *50*, 2649.

(19) Tang, B. Z.; Geng, Y.; Lam, J. W. Y.; Li, B.; Jing, X.; Wang, X.; Wang, F.; Pakhomov, A. B.; Zhang, X. *Chem. Mater.* **1999**, *11*, 1581.

(20) Demas, J. N.; Grosby, G. A. *J. Phys. Chem.* **1971**, *75*, 991.

(21) Dong, S.; Li, Z.; Qin, J. *J. Phys. Chem. B* **2009**, *113*, 434.

(22) Haidekker, M. A.; Theodorakis, E. A. *Org. Biomol. Chem.* **2007**, *5*, 1669.

(23) (a) Hong, Y.; Chen, S.; Leung, C. W. T.; Lam, J. W. Y.; Liu, J.; Tseng, N. W.; Kwok, R. T. K.; Yu, Y.; Wang, Z.; Tang, B. Z. *ACS Appl. Mater. Interfaces* **2011**, *3*, 3411. (b) Bhalla, V.; Vij, V.; Dhir, A.; Kumar, M. *Chem.—Eur. J.* **2012**, *18*, 3765.

(24) Gampp, H.; Maeder, M.; Meyer, C. J.; Zubberbulher, A. D. *Talanta* **1985**, *32*, 95.

(25) Olley, D. A.; Wren, E. J.; Vamvounis, G.; Fernee, M. J.; Wang, X.; Burn, P. L.; Meredith, P.; Shaw, P. E. *Chem. Mater.* **2011**, *23*, 789.

(26) A comparison of the selectivity, K_{SV}, and detection limit of the **5**-Hg^{2+} ensemble with previous reports is given in Supporting Information, Table S1.

(27) Sohn, H.; Sailor, M. J.; Magde, D.; Trogler, W. C. *J. Am. Chem. Soc.* **2003**, *125*, 3821.

(28) Kaur, I.; Jia, W.; Kopreski, R. P.; Selvarasah, S.; Dokmeci, M. R.; Pramanik, C.; McGruer, N. E.; Miller, G. P. *J. Am. Chem. Soc.* **2008**, *130*, 16274.

(29) (a) Yang, J. S.; Swager, T. M. *J. Am. Chem. Soc.* **1998**, *120*, 5321. (b) Thomas, S. W.; Amara, J. P.; Bjork, R. E.; Swager, T. M. *Chem. Commun.* **2005**, 4572.

(30) (a) Albert, K. J.; Lewis, N. S.; Schauer, C. L.; Sotzing, G. A.; Stitzel, S. E.; Vaid, T. P.; Walt, D. R. *Chem. Rev.* **2000**, *100*, 2595. (b) Kim, T. H.; Lee, B. Y.; Jaworski, J.; Yokoyama, K.; Chung, W. -J.; Wang, E.; Hong, S.; Majumdar, A.; Lee, S.-W. *ACS Nano* **2011**, *5*, 2824.